Title:

Thermal stress triggers productive viral infection of a key coral reef symbiont

Running title:

Dynamics of dinoRNA viruses in heat-stressed coral colonies

Authors and affiliations:

Carsten GB Grupstra[1], Lauren I Howe-Kerr[1]*, Alex J Veglia[1]*, Reb L Bryant[1,2], Samantha R Coy[1], Patricia L Blackwelder[3], Adrienne MS Correa[1]

[1]BioSciences at Rice, Rice University, Houston, TX, USA.

[2]Department of Ecology and Evolutionary Biology, The University of Kansas, Lawrence, KS, USA.

[3]University of Miami Center for Advanced Microscopy (UMCAM), Department of Chemistry, 1301 Memorial Dr, Coral Gables, FL 33146-0630, USA

*These authors contributed equally to this work.

Competing Interests statement:

The authors declare that they have no competing interests.

Abstract

Climate change-driven ocean warming is increasing the frequency and severity of bleaching events, in which corals appear whitened after losing their dinoflagellate endosymbionts (family Symbiodiniaceae). Viral infections of Symbiodiniaceae may contribute to some bleaching signs, but little empirical evidence exists to support this hypothesis. We present the first temporal analysis of a viral lineage—the Symbiodiniaceae-infecting 'dinoRNAVs'—in coral colonies exposed to a 5-day heat treatment. Throughout the experiment, all colonies were dominated by Symbiodiniaceae in the genus *Cladocopium*, but 124 dinoRNAV major capsid protein 'aminotypes' (unique amino acid sequences) were detected across coral genets and treatments. Seventeen dinoRNAV aminotypes were found only in heat-treated fragments, and 22 aminotypes were detected at higher relative abundances in heat-treated fragments. DinoRNAVs also exhibited higher alpha diversity and dispersion under heat stress. Together, these findings provide the first empirical evidence that exposure to high temperatures triggers some dinoRNAVs to switch from a persistent to a productive infection mode within heat-stressed corals. Over extended time frames, we hypothesize that cumulative dinoRNAV lysis of Symbiodiniaceae cells during productive infections could decrease Symbiodiniaceae densities within corals, observable as bleaching signs. This study sets the stage for reef-scale investigations of dinoRNAV dynamics during bleaching events.

Introduction

Warming seas, driven by climate change, are increasingly causing bleaching events: mass losses of endosymbiotic dinoflagellates (family Symbiodiniaceae) from corals and other invertebrate hosts. Bleaching events often result in coral mortality and are contributing to the degradation of reef ecosystems globally (1,2). Viruses, which are diverse and abundant on coral colonies (3–7), are hypothesized to contribute to some coral bleaching signs by lysing Symbiodiniaceae cells (e.g. 8–10). Alternatively, viral shifts in conjunction with bleaching-associated stressors (11,e.g. 12–14) could merely be correlated with bleaching signs or constitute opportunistic secondary infections (15,16). Beyond bleaching, viruses may influence colony health by altering the function of resident microbial symbionts or coral tissues (e.g. 17–23). Although various roles for viruses in coral bleaching, disease and function have been hypothesized, thus far, these roles have been difficult to test empirically.

Symbiodiniaceae are putative target hosts of DNA and RNA viruses (reviewed in 6,7), including the 'dinoRNAVs', a group of dinoflagellate-infecting positive-sense single stranded RNA viruses. Although dinoRNAVs have yet to be isolated, stably propagated, and fully characterized, they have been detected from Symbiodiniaceae cultures, as well as Atlantic and Pacific corals spanning 6 genera (Table 1). These associations suggest that dinoRNAVs are prevalent as persistent infections in Symbiodiniaceae cells (8–10,24,25). Furthermore, increased dinoRNAV detection (24) and enhanced host anti-viral response (26) suggest that under stressful conditions, dinoRNAVs may switch to a more productive replication mode in which they directly lyse their hosts. This infection strategy has recently been identified in other algal host-virus systems (e.g., coccolithophore Emiliana huxleyi-EhV system, 27).

Heterocapsa circularisquama RNA virus (HcRNAV), which infects free-living dinoflagellates, is among the closest known relatives to Symbiodiniaceae-infecting dinoRNAVs (24,28). HcRNAV undergoes a strictly lytic replication cycle following a latent period of 24-48 hours, during which the host is infected but not lysed and viruses have not been released (29). We therefore posited that shifts by Symbiodiniaceae-infecting viruses into a more productive replication mode might also be detectable within the first few days of exposure to stress (13,24,26). Examining viral dynamics within individual colonies at the onset of thermal stress should clarify the relationship between viral infection of Symbiodiniaceae and coral bleaching signs.

To investigate the role of Symbiodiniaceae-infecting viruses in coral bleaching, we quantified, for the first time, the temporal dynamics of dinoRNAVs within individual coral colonies. To accomplish this, colonies of the stony coral *Pocillopora* species complex were exposed to acute (+~2ºC) thermal stress, and dinoRNAV diversity was quantified over a 5-day period. We hypothesized that: (1) dinoRNAVs are common in coral colonies; (2) dinoRNAV richness increases and compositions shift under thermal stress; and (3) changes to dinoRNAVs occur within 72 hours. By analyzing dinoRNAV diversity at the amino acid level, this study partially circumvented methodological challenges arising from the high mutation rates and genetic diversity of single-stranded RNA viruses (30–32), which have previously made it difficult to compare RNA viral dynamics across ecologically relevant scales (33). As dinoRNAV work on reefs continues to progress, the aminotypes presented here may eventually merit further collapse into ‘quasispecies’—heterogeneous mixtures of related genomes (33–36)—a common approach for conceptualizing diversity within RNA virus populations.

Materials and methods

Experimental design

We conducted a replicated aquarium experiment (two treatments; four aquariums per treatment) in which fragments from five colonies of *Pocillopora* species complex (37) were exposed to control conditions (ambient reef water; 28.2˚C) or a +2.1˚C heat treatment (summer bleaching temperatures; 30.3˚C) for 5 days (See Figure S1 and Supplementary Methods, 38,39). At the start of the experiment ($t_{(h)}$ = 0), all fragments were photographed with a Coral-Watch Health Monitoring Chart (40) in the frame, and one fragment per colony in the control aquaria was preserved as an initial control. At five time points ($t_{(h)}$ = 4, 12, 24, 72 and 108 h), all fragments were photographed again and visually inspected for signs of stress (e.g., excessive mucus production), lesions and/or paling. A control and a heat-stressed fragment per colony were also preserved at each time point (generating 10 fragments per time point). DNA and RNA were extracted from each sample (which included coral animal tissue, Symbiodiniaceae cells and viruses) using a ZymoBIOMICS DNA/RNA Miniprep Kit (Zymo Research, Irvine, CA, USA) with an additional enzyme digestion step to improve viral RNA yields; cDNA was then synthesized from eluted RNA (see Supplementary Methods). At the 24 and 72 h timepoints, samples were also fixed for transmission election microscopy (TEM) imaging in 3X PBS with 2% paraformaldehyde (see Supplementary Methods).

To characterize the effect of the heat treatment on Symbiodiniaceae cell densities (a metric of coral health and bleaching status), we compared brightness values from standardized photographs of each coral fragment—a proxy for Symbiodiniaceae chlorophyll concentrations—at the start of the experiment and at the time of preservation (see Supplementary Methods, 40,41). Symbiont diversity was characterized by sequencing the internal transcribed spacer-2 (ITS-2) region of Symbiodiniaceae rDNA from fragments of each coral colony using primers

from Hume et al (42) following methods in Howe-Kerr et al (43; see Supplementary Methods). Sequences were processed using Symportal (44).

Sequencing of dinoRNAV major capsid protein gene amplicons, bioinformatics processing, and phylogenetic analysis

The dinoRNAV major capsid protein (*mcp*) gene was amplified from cDNA libraries using a nested PCR protocol with degenerate primers (28); cleaned and normalized libraries were sequenced on the Illumina MiSeq platform using PE300 v3 chemistry. Processing and analysis of dinoRNAV *mcp* gene reads was conducted using the program vAMPirus (See Supplementary Methods for sequencing and read processing details; Veglia *et al.*, 2021). Briefly, ASVs were generated using the UNOISE (46) algorithm with vsearch (47), and all ASVs were then translated and collapsed into unique amino acid sequences, 'aminotypes'. Any sequences containing stop codons were removed prior to further analysis.

An alignment was made in MUSCLE using aminotypes from this study, a dataset from the Great Barrier Reef (28) that was reprocessed using the methods above, and a set of reference best BLASTx hits to the NCBI database (48). The alignment (Supplementary Data 1) was trimmed to the first column on either side which contained no gaps, and then used to determine the best model for evolution (LG+G4+I) according to ModelTest-NG (49). A maximum-likelihood phylogeny was inferred with RAxML-NG (1000 bootstrap iterations) and rooted with HcRNAV as an outgroup.

DinoRNAV diversity metrics based on *mcp* aminotypes

All data processing, visualization, analysis and statistical tests were conducted in R version 4.0.2 and Vegan 2.5-6 (50) on an aminotype counts table (Supplementary Data 2). For some analyses, the dataset was rarefied to 59 837 amino acid sequences. Shannon's diversity index (H) values

were calculated based on rarefied data; expected aminotype richness values were calculated using repeated random subsampling of non-rarefied data (sample size=59 837 amino acid sequences). Venn diagrams were made from non-rarified data using the online tool http://bioinformatics.psb.ugent.be/webtools/Venn/ (accessed August 17th, 2020). For comparison, Venn diagrams were also made based on rarified data (results not shown); these Venn diagrams exhibited similar patterns but were less conservative and were therefore not included.

To quantify the dispersion of dinoRNAVs between treatments and over time, a non-metric multidimensional scaling (NMDS) plot was constructed based on Bray-Curtis distances from square-root-transformed rarefied data (k=2, 999 iterations), and the distance to centroid for each sample was calculated. Since dinoRNAVs differed among coral colonies, we calculated centroids for each individual colony in the control and heat treatments separately (5 colonies x 2 treatments = 10 centroids) in order to examine the effect of heat treatment on dinoRNAV dispersion in a given coral colony. For this analysis, different timepoints were used as replicates.

Statistical analyses

We tested for differences in brightness values from the coral fragment colorimetric analysis, as well as differences in dinoRNAV aminotype alpha diversity (Shannon's index and aminotype richness) and dispersion (distance to centroid) using linear mixed effects models (LMM) with the package LME4 v1.1-23 (40,51). We tested for an interaction between treatment and timepoint; by incorporating colony ID as a random effect, this analysis approaches a repeated measures test. F-tests were used for model selection with car v3.0-8. Assumptions of normality of the residuals were assessed visually with quantile-quantile plots and Shapiro-Wilk tests; the assumption of homogeneity of variance was visually assessed using plots with residuals

versus fitted values. Dispersion values did not follow the assumption of normality of the residuals and were square root-transformed. We also tested for differences between control and heat-treated fragments at each timepoint (using colonies as replicates), as well as per colony (using time points as replicates), on dinoRNAV aminotype diversity and dispersion with ANOVAs and controlled for type 1-errors using a Bonferroni correction.

The effect of heat treatment on the overall composition of dinoRNAVs was tested with a PERMANOVA using adonis() in vegan based on Bray-Curtis distances from square-root-transformed rarefied data. We tested for an interaction between treatment and colony and added time as an additional factor. Although dispersion differed significantly among groups (betadisper test), PERMANOVA is robust to heterogeneous dispersion if the design is balanced (52).

Lastly, we conducted a differential abundance analysis using the non-rarefied amino acid counts table with DESeq2 v1.26.0 (53). We fitted a negative binomial model and Benjamini-Hochberg FDR-corrected Wald tests (α=0.05) were used to test for differences in taxon abundance between treatment within each colony and at each timepoint after the start of the experiment ($t_{(h)}$= 4, 12, 24, 72, 108). We excluded all fragments sampled at timepoint 0 and any fragments with <10 000 reads, as well as the fragment from the other treatment corresponding to the fragment with insufficient reads at the same time (colonies 3 and 5 at timepoint $t_{(h)}$=4, colony 3 at $t_{(h)}$=72).

Results

Coral holobiont traits

Coral fragments in the control and heat aquariums remained apparently healthy throughout the experiment; no signs of stress such as paling, mucus production, or tissue sloughing were observed. Linear mixed effects models of color values did not reveal significant paling in heat-

treated coral fragments (treatment F=0.10, p=0.75; timepoint F= 0.30, p=0.59; treatment*timepoint F= 0.09, p= 0.77). Lack of color change was expected; bleaching signs are generally only detectable after weeks of ecologically relevant temperature stress—even though vital molecular processes are affected after several days (54). All colonies contained what we interpret as a species of Symbiodiniaceae closely related to *Cladocopium goreaui* (44,55); Symbiodiniaceae diversity did not change over time (Figure S2).

Transmission electron microscopy imaging of Symbiodiniaceae and associated virus-like particles

Symbiodiniaceae cells in coral fragments exposed to 24 hours of heat treatment showed a pattern of vacuolization in the chloroplasts (Figure 1a) compared to cells in control fragments (Figure 1g). Many vacuoles in Symbiodiniaceae cells contained one to several VLPs with icosahedral, electron-dense capsids that were 110-170 nm in size and lacking envelopes (Figure 1a-d). Similar VLPs were observed immediately outside Symbiodiniaceae cells; some also appeared to be endocytosed by—or exiting out of—Symbiodiniaceae cells (Figure 1e-h).

DinoRNAV major capsid protein (*mcp*) gene sequencing overview

Amplicon sequencing of the dinoRNAV major capsid protein (*mcp*) gene resulted in 10 222 055 paired raw reads from all samples and one negative control. A total of 7 593 537 reads with a mean length of 423 bases (before trimming to 422 bases) remained after merging and quality control. Denoising resulted in 273 unique amplicon sequence variants (ASVs) across all samples, and translation revealed that 11 ASVs contained stop codons; these ASVs were removed. Translated ASVs collapsed into 124 ‘aminotypes’ (unique amino acid sequences) at a length of 140 amino acids.

DinoRNAV *mcp* genes were detected in fragments from all 5 coral colonies, but 5 control samples and the negative control were not retained for further analysis because they contained few (<10 000) amino acid sequences (the negative control had 20 amino acid sequences). All remaining samples had between 50 000 and 210 000 amino acid sequences with a mean read depth of 142 810 ± 36 163 (SD).

DinoRNA viruses in *Pocillopora* species complex colonies are closely related to dinoRNAVs in other coral species

The 124 unique dinoRNAV aminotypes (Figure 2; Table S1) identified in this study were most similar to 13 amino acid sequences from a previously published dinoRNAV library (28); sequence similarities to aminotypes from published dinoRNAVs ranged from 52.1-99.3% (e-values ranged between $9.6 \cdot 10^{-73}$-$2.7 \cdot 10^{-35}$, Table S1). All dinoRNAV *mcp* aminotypes in this study form a clade that is more recently derived than reference sequences such as HcRNAV, Beihai sobemo-like virus and sponge weivirus-like virus (Figure 2). The dinoRNAV aminotypes in this study may form (at least) three quasispecies (e.g. red rectangles in Figure S3, sensu 56). Strikingly, the majority of dinoRNAV *mcp* genes identified in our study occupy one clade; on average, sequences in this clade vary 9.8% ± 5.5 (SD) from each other (Figure 2; Figure S3). Ultra-deep sequencing may be necessary to further clarify the drivers of these potential 'mutant cloud dynamics' in Symbiodiniaceae hosts (57). In several branches of the tree, aminotypes from our study are most closely related to aminotypes detected from Symbiodiniaceae in *Acropora tenuis, Favia fungites, Galaxea fascicularis, Pocillopora damicornis, Porites cylindrica,* and *Porites lutea* corals sampled from the Great Barrier Reef (28). Dominant aminotypes (>1% abundance across total dataset) are present in all major branches of the tree but differ by as much

as ~40% in amino acid sequence (Supplementary Figure 3). Aminotypes detections varied across treatment and time in the experiment (shading of red and black squares in Figure 2).

DinoRNAV aminotypes differed among coral colonies and treatments

Approximately 34% (42 of 124 aminotypes) of aminotypes in this study were present in all colonies, 48% (60) were shared between 2-4 colonies and 18% (22) were unique to individual coral colonies (with individual colonies having up to 6 unique colony-specific aminotypes, Figure 3a). All 14 aminotypes that each comprised >1% reads in the total dataset (listed in Figure 3b) were detected in all five coral colonies. DinoRNAV aminotypes varied among individual colonies (Figure 3b); colony ID was the most powerful predictor of viral composition (PERMANOVA: R^2 = 0.76, $p<0.001$). DinoRNAVs responded to elevated temperatures in colony-specific ways, as indicated by a significant interaction effect between treatment and colony (PERMANOVA: R^2=0.068, $p<0.001$). Treatment was also significant by itself (PERMANOVA: R^2= 0.02, $p<0.001$), demonstrating a subtle but consistent response to elevated temperatures across all colonies. Time was not a significant predictor (PERMANOVA: R^2= 0.01, p=0.77; Figure 3b).

Heat treatment rapidly increased the diversity of dinoRNAV aminotypes

A total of 17 aminotypes were unique to the heat treatment; 1 aminotype was unique to the controls (Figure 4a; Table 2). Heat-specific aminotypes were observed in all colonies and ranged from 1-6 unique aminotypes per colony. Three heat-specific aminotypes were shared among multiple (2-3) coral colonies; the remaining 14 heat-specific aminotypes were not shared between colonies. These findings demonstrate that heat-specific aminotypes were not restricted to individual fragments but were shared between fragments of the same colony or among

colonies. However, most heat-specific aminotypes were relatively rare, with only two aminotypes comprising >1% of reads in each fragment (aminotypes 25 with 1.8%; aminotype 114 with 1.4%; other aminotypes with means of 0.01-0.7% of reads in individual fragments). The single aminotype that was unique to control fragments was identified in one fragment after 72 hours (0.02% of reads in that fragment).

Alpha diversity (Shannon's index, H) of aminotypes was positively associated with the heat treatment ($F=4.92$, $p=0.03$) and time ($F=4.86$, $p=0.03$) in our linear mixed effects model (LMM; Figure 4b, d, h). There was no significant interaction between heat and time ($F=0.54$, $p=0.47$). On average (± SE), Shannon's index was 27% higher in heat-treated fragments (1.1 ± 0.6) than controls (0.8 ± 0.6; Figure 4b). Within individual timepoints, heated fragments had 4-93% higher mean H values (0.9-1.3) than controls (0.7-1.0; Figure 4d), but individual comparisons were not significant. Means of Shannon's index per colony ranged between 0.1-1.6 for control fragments and 0.5-1.8 for heat-treated fragments (Figure 4f).

There was a significant positive association between viral aminotype richness and heat treatment ($F=5.71$, $p=0.02$), but not aminotype richness and time ($F=0.36$, $p=0.55$) in our LMM (Figure 4c, e, i). There was no significant interaction between treatment and time ($F=0.10$, $p=0.75$). On average, aminotype richness was 16% higher in heat-treated (37.2 ± 2.0) than control fragments (32.0 ± 2.1; Figure 4c). At individual timepoints, heat-treated fragments had 7-23% higher mean aminotype richness (34.8-39.1) than controls (29.2-35.4; Figure 4e), but these differences were not significant. Mean aminotype richness for individual colonies (using timepoints as replicates) ranged between 19.5-44.6 for control fragments and 28.0-44.9 for heat-treated fragments (Figure 4g).

Twenty-two aminotypes had higher relative abundances in heat-treated fragments

DESeq2 analysis revealed 28 aminotypes had significantly altered relative abundances in heat-treated or control fragments (Figure 5). Twenty-two aminotypes had higher relative abundances in heated fragments, whereas 6 aminotypes had higher relative abundances in controls. Ten aminotypes were differentially abundant at multiple (2-4 out of 5) timepoints throughout the experiment. Aminotypes 29, 38 and 98 were significantly more abundant in the heat treatment in 4 out of 5 sampled timepoints (from 12 to 108 h); Aminotype 93 was more abundant in the final 3 timepoints (from 24 to 108 h).

Dispersion of dinoRNAV *mcp* amino acid sequences increased in heat-treated fragments

Dispersion (measured as distance to centroid) of dinoRNAVs was positively associated with heat treatment (Figure 6a, b, e; $F=11.00$, $p=0.002$) in our LMM. There was no effect of time ($F=1.07$, $p=0.31$) and no interaction between treatment and time ($F=0.64$, $p=0.43$). Overall, mean (±SE) dispersion was 62% higher in the heat treatment when all colonies and timepoints were pooled (control: 0.14 ± 0.09; heat: 0.23 ± 0.13). A trend of increasing dispersion (32-100% higher) of dinoRNAVs was observed in heat-treated samples at individual timepoints (Figure 6c; controls: 0.12-0.17; heat: 0.2-0.29), but individual comparisons were not significant. Mean dispersion of individual colonies (across timepoints) ranged between 0.1-0.24 for controls and 0.13-0.37 for heat-treated fragments, resulting in an increase of 11-93% per colony, but individual comparisons were not significant (Figure 6d).

Discussion

Viruses can have diverse impacts on hosts, ranging from antagonistic to beneficial (58–61). Efforts to understand how viral infections impact coral colonies have been stymied by the lack of (1) a high-throughput approach to track a viral lineage in colonies across an acute stress event; and (2) established cultures of viruses associated with corals (for use in viral addition experiments). This study tracks a group of Symbiodiniaceae-infecting viruses, the dinoRNAVs, in a controlled experiment to interrogate how infection responds to temperatures associated with bleaching. DinoRNAVs were detected from all five coral colonies examined, and from every heat-treated coral fragment, but only some controls. These observations, as well as detections of higher alpha diversity of *mcp* aminotypes, increased dinoRNAV dispersion, the identification of unique *mcp* aminotypes, and greater relative abundances of specific aminotypes in heat-treated fragments, together strongly indicate that dinoRNAV infections were more active in heat-treated fragments. DinoRNAV responses were detectable within a single day, more quickly than the several weeks over which bleaching signs typically manifest. If viral infection of Symbiodiniaceae cells is enhanced (e.g., increased production, accumulation of viral diversity) during thermal anomalies *in situ*, then this cumulative viral activity (if maintained over weeks) could contribute to bleaching onset on reefs, or otherwise disrupt of coral-Symbiodiniaceae partnerships.

DinoRNAVs as a common, persistent virus of Symbiodiniaceae

DinoRNAV *mcp* genes were detected in all colonies (N=5), and in most to all fragments per colony (73-100% of fragments, N=8/11 – 11/11 fragments per colony). DinoRNAV genes have additionally been reported from colonies of seven other stony coral species across the Atlantic and Pacific Oceans (Table 1, Figure 2), suggesting that these viruses are commonly associated with coral microbiota. In this experiment, viral aminotype compositions (and potential viral

quasispecies) differed among coral colonies, but were similar within the fragments of a given colony, despite maintenance in separate aquaria (Figure 3). These results suggest that, under ambient conditions, dinoRNAV populations are driven strongly by within-colony factors and are relatively homogeneously distributed throughout entire coral colonies. RNA viruses rely on RNA-dependent RNA polymerase (RdRp) for replication, which is relatively error-prone. Therefore, individual viral progenitors infecting Symbiodiniaceae cells in a given colony may each produce a variety of genetically distinct viral "progeny" during a single replication cycle (34,62); hence, the observed pattern of colony-specificity in dinoRNAV aminotypes likely results from diversification within 'quasispecies' and (potentially) subsequent purifying selection (33,63–65). This production of a 'mutant cloud' of dinoRNAV diversity may even help ensure these viruses are successful (at the population level) at infecting Symbiodiniaceae under changing environmental conditions (35).

Healthy corals contain millions of Symbiodiniaceae cells per cm^2 of coral tissue; our results suggest that Symbiodiniaceae cells *in hospite* may be infected by one or perhaps several dinoRNAV quasispecies at any given time (e.g., Symbiodiniaceae in colonies 2 and 3, Figures 2 and 3). Recent surveys of free-living marine microbial communities reported that viral infections may occur in ~33% (66,67) to over 60% (68) of marine microorganisms, and many individual cells may be infected by several viruses at a given time (66,69). Considering that our sequencing data are based on *mcp* gene amplicons from RNA libraries generated from unfractionated coral tissue, dinoRNAV *mcp* gene detections could potentially arise from several sources, including RNA genomes within intact dinoRNAV capsids (28), *mcp* genes that are being expressed in host cells during the dinoRNAV replication cycle, free dinoRNAV genomes that may occur as extrachromosomal RNA in a latent (25) or carrier state similar to pseudolysogeny (70,71), and/or

expressed endogenized viral elements in host genomes (72,73). The amplicon sequencing approach employed here limits our ability to discern amongst these potential sources of viral *mcp* gene detections, as does the dearth of information available on dinoRNAV replication cycles. Approaches such as single cell RNA-seq (e.g. 74) of Symbiodiniaceae cells, as well as sequencing methods designed to identify and characterize infective viruses (similar to viral tagging, 75,adsorption sequencing, 76) represent critical next steps in assessing the prevalence of dinoRNAV infections within individual Symbiodiniaceae cells, and the provenance of dinoRNAV *mcp* gene detections (e.g RNA genomes from intact viruses vs *mcp* genes expressed during the replication cycle), respectively.

Switching from persistent to more productive infection under stress

Marine viruses have diverse infection strategies; many viruses switch between strategies upon environmental changes (58,77–81). Some marine viruses, for example, may switch between latent and productive cycles upon a variety of host-related or environmental triggers (8,82,83). RNA virus infections can range from exclusively lytic (29,84,85), to infections that are 'persistent' or 'chronic' and do not immediately kill the host (86,87). Persistent RNA viruses of plants, for example, may show altered activity based on seasonality (88), temperature (89,90), or other environmental factors (90). For persistent viruses of Symbiodiniaceae, a variety of mechanisms may modulate viral infection strategies; the role of temperature in triggering persistent infections to become more productive has received particular attention due to the link between high temperature and coral bleaching (8,24,26,83,91).

We identified 22 aminotypes that were present at higher relative abundances in heat-treated coral fragments (Figure 5), and 17 aminotypes were unique to these fragments (Figure 4a, c). We hypothesize that these findings indicate a switch from persistent to more productive

354 infections by some dinoRNAV strains (or quasispecies). In this study, aminotypes 29, 38, 93 and
355 98 are particular candidates for this hypothesis, given their sustained relative increase in
356 abundance in heat-treated corals starting at 12-24 hours (Figure 5). We encourage future studies
357 to screen corals and Symbiodiniaceae communities (and existing sequencing libraries) for these
358 aminotypes.

359 The observation of a rapid increase in dinoRNAV aminotypes diversity during the onset
360 of thermal stress is consistent with a previous report of increased (but overall low) abundance of
361 dinoRNAV transcripts in the Caribbean coral *Montastrea cavernosa* following exposure to
362 elevated temperatures for 12 hours (24). Further, a thermosensitive culture of Symbiodiniaceae
363 C1 had high expression of dinoRNAVs under ambient temperatures, suggesting that dinoRNAV
364 may modulate resistance to bleaching in some species or populations of Symbiodiniaceae (26).
365 Similarly, viral metagenomes from bleached pocilloporid colonies *in situ* contained significantly
366 more eukaryotic virus sequences than unbleached, apparently healthy colonies (12). Experiments
367 with the cricket paralysis virus—a +ssRNAV with similar genome architecture to dinoRNAVs in
368 Symbiodiniaceae cultures—also showed increased viral replication after two hours when
369 temperatures were raised by 5 ºC (92). Taken together, our findings and those from other studies
370 indicate that dinoRNAVs may play key roles in altering the thermal sensitivity of
371 Symbiodiniaceae, and perhaps, coral colonies.

372 **Virus-like particles associated with heat-stressed Symbiodiniaceae cells**

373 After 24 hours of heat treatment, virus-like particles (VLPs) 110-170 nm in diameter were
374 observed in vacuoles within Symbiodiniaceae cells (Figure 1). These VLPs were similar in size
375 members of the *Phycodnaviridae*, such as *Chloroviruses*, *Coccolithoviruses*, and *Prasinoviruses*,
376 within the nucleocytoplasmic large DNA viruses (NCLDVs). These viral groups have been

previously reported from cultured Symbiodiniaceae cells via metagenomic approaches (26) and from Symbiodiniaceae *in hospite* through a combination of metagenomic analysis and TEM imaging (12,13). We observed VLPs that may have been entering or exiting Symbiodiniaceae cells (Figure 1), suggesting active infections were occurring. Such observations—concurrent with genetic shifts in dinoRNAVs—corroborate that diverse viral groups likely respond to increased temperatures (8,10,91,93,94).

RNA viruses known to infect free-living dinoflagellates, such as HcRNAV, have icosahedral capsids ~30 nm in diameter (29). Similarly sized VLPs were not observed in this study, but the capsid morphology of Symbiodiniaceae-infecting dinoRNAVs remains unconfirmed. Isolation of Symbiodiniaceae-infecting dinoRNAVs and characterization of their replication cycle will further clarify which VLPs in Symbiodiniaceae TEM images are potential dinoRNAVs.

Colony-specific dinoRNAV responses to elevated temperatures

Since higher temperatures increase host cell enzymatic activity, increased viral production and accumulation of mutations within quasispecies exposed to heat stress might be expected based on thermodynamics alone (95). However, dinoRNAV responses to elevated water temperatures differed among individual coral colonies (Figures 3b, 6a), even in two colonies (3 and 4) that were both dominated by aminotype 1 in control aquaria. While dinoRNAVs in heat-treated fragments from colonies 1 and 3 exhibited strong shifts in putative quasispecies compositions, such changes were less pronounced in the other colonies. These findings suggest colonies 1 and 3 and/or their dinoRNAV quasispecies were more sensitive to heat stress. Coral colonies generally exhibit heterogeneous resistance to coral bleaching (e.g. 96,97), and bleaching susceptibility in *Pocillopora* species complex has been correlated to differential communities of

eukaryotic viruses (12). Taken together, we hypothesize that colonies 1 and 3 in our study were more sensitive to temperature stress and likely would have shown signs of bleaching had the experiment run longer. Subsequent experiments that extend multiple weeks to sample both the onset of thermal stress and the onset of bleaching signs are a critical next step in understanding how dinoRNAV dynamics relate to colony health trajectories and relative bleaching resistance.

Conclusions

This is the first study to characterize the dynamics of Symbiodiniaceae-infecting dinoRNAVs in coral colonies exposed to ecologically relevant bleaching temperatures. We identified dinoRNAVs in each sampled coral; temperature stress elicited rapid changes to potential dinoRNAV quasispecies in terms of diversity and composition, and a subset of viral aminotypes were significantly associated with heat-treated corals. Together, these multiple lines of evidence suggest that dinoRNAVs are common as persistent infections of Symbiodiniaceae. Environmental stress may increase the productivity of these viruses, contributing to bleaching signs or other impacts on coral-Symbiodiniaceae partnerships (if stress is prolonged). Overall, these findings add to the growing body of literature demonstrating that viruses of microorganisms affect emergent phenotypes of animal and plant holobionts, and may modulate holobiont responses to changing environmental conditions.

Acknowledgements

The authors extend their sincere appreciation to Drs. Rebecca L. Vega Thurber, Andrew R. Thurber, and Craig E. Nelson for input on, and help with setting up, the experiment. Many thanks to Rebecca L. Maher and J. Grace Klinges for help with sampling, and to Dennis Conetta for assistance with DNA and RNA extractions. We additionally thank Mark Dasenko at Oregon

State University's Center for Genome Research & Biocomputing (Corvallis, OR) for his support in designing the sequencing methods. Financial support was provided by a Sigma-Xi Grant-in-aid of Research to C.G., a U.S. National Science Foundation award (OCE #1635798) to A.M.S.C. and an Early-Career Research Fellowship (#2000009651) from the Gulf Research Program of the National Academies of Sciences to A.M.S.C.

Author contributions

C.G., L.H.K. and A.C. conceived of the experiment; C.G., L.H.K., and A.J.V. developed the methods with support from A.C.; C.G., L.I.H., R.B., and A.C. conducted the experiments and processed samples; C.G. led data analysis, with contributions by all authors; C.G. wrote the first draft of the manuscript, with contributions by all authors.

References

1. Hughes TP, Kerry J, Álvarez-Noriega M, Álvarez-Romero J, Anderson K, Baird A, et al. Global warming and recurrent mass bleaching of corals. Nature. 2017;

2. Hoegh-Guldberg O. Climate change, coral bleaching and the future of the world's coral reefs. Mar Freshw Res. 1999;50:839–66.

3. Patten NL, Harrison PL, Mitchell JG. Prevalence of virus-like particles within a staghorn scleractinian coral (Acropora muricata) from the Great Barrier Reef. Coral Reefs. 2008;27(3):569–80.

4. Leruste A, Bouvier T, Bettarel Y. Enumerating viruses in coral mucus. Appl Environ Microbiol. 2012;78(17):6377–9.

5. Nguyen-Kim H, Bettarel Y, Bouvier T, Bouvier C, Doan-Nhu H, Nguyen-Ngoc L, et al. Coral mucus is a hot spot for viral infections. Appl Environ Microbiol. 2015;81(17):5773–83.

6. Vega Thurber R, Payet JP, Thurber AR, Correa AMS. Virus–host interactions and their roles in coral reef health and disease. Nat Rev Microbiol [Internet]. 2017;15:205–16. Available from: http://www.nature.com/doifinder/10.1038/nrmicro.2016.176

7. Sweet M, Bythell J. The role of viruses in coral health and disease. J Invertebr Pathol [Internet]. 2017;147:136–44. Available from: http://dx.doi.org/10.1016/j.jip.2016.12.005

8. Wilson WH, Francis I, Ryan K, Davy SK. Temperature induction of viruses in symbiotic dinoflagellates. Aquat Microb Ecol. 2001;25(1):99–102.

9. Lohr J, Munn CB, Wilson WH. Characterization of a latent virus-like infection of symbiotic zooxanthellae. Appl Environ Microbiol. 2007;73(9):2976–81.

10. Lawrence SA, Wilson WH, Davy JE, Davy SK. Latent virus-like infections are present in a diverse range of Symbiodinium spp. (Dinophyta). J Phycol. 2014;50(6):984–97.

11. Marhaver KL, Edwards RA, Rohwer F. Viral communities associated with healthy and bleaching corals. Environ Microbiol. 2008;10(9):2277–86.

12. Messyasz A, Rosales SM, Mueller RS, Sawyer T, Correa AMS, Thurber AR, et al. Coral Bleaching Phenotypes Associated With Differential Abundances of Nucleocytoplasmic Large DNA Viruses. Front Mar Sci. 2020;7(October):1–15.

13. Correa AMS, Ainsworth TD, Rosales SM, Thurber AR, Butler CR, Vega Thurber RL. Viral outbreak in corals associated with an in situ bleaching event: Atypical herpes-like viruses and a new megavirus infecting symbiodinium. Front Microbiol. 2016;7(FEB):1–14.

14. Bettarel Y, Thuy NT, Huy TQ, Hoang PK, Bouvier T. Observation of virus-like particles in thin sections of the bleaching scleractinian coral Acropora cytherea. J Mar Biol Assoc United Kingdom. 2013;93(4):909–12.

15. Lesser MP, Bythell JC, Gates RD, Johnstone RW, Hoegh-Guldberg O. Are infectious diseases really killing corals? Alternative interpretations of the experimental and ecological data. J Exp Mar Bio Ecol. 2007;346(1–2):36–44.

16. Soffer N, Brandt ME, Correa AMS, Smith TB, Thurber RV. Potential role of viruses in white plague coral disease. ISME J [Internet]. 2014;8(2):271–83. Available from:

http://dx.doi.org/10.1038/ismej.2013.137

17. Lawrence SA, Davy JE, Aeby GS, Wilson WH, Davy SK. Quantification of virus-like particles suggests viral infection in corals affected by Porites tissue loss. Coral Reefs. 2014;33:2014.

18. Lawrence SA, Davy JE, Wilson WH, Hoegh-Guldberg O, Davy SK. Porites white patch syndrome: associated viruses and disease physiology. Coral Reefs. 2015;34(1):249–57.

19. Pollock FJ, M. Wood-Charlson E, Van Oppen MJH, Bourne DG, Willis BL, Weynberg KD. Abundance and morphology of virus-like particles associated with the coral Acropora hyacinthus differ between healthy and white syndrome-infected states. Mar Ecol Prog Ser. 2014;510(June):39–43.

20. Vega Thurber RL, Correa AMS. Viruses of reef-building scleractinian corals. J Exp Mar Bio Ecol [Internet]. 2011;408(1–2):102–13. Available from: http://dx.doi.org/10.1016/j.jembe.2011.07.030

21. Weynberg KD, Voolstra CR, Neave MJ, Buerger P, Van Oppen MJH. From cholera to corals: Viruses as drivers of virulence in a major coral bacterial pathogen. Sci Rep. 2015;5:1–9.

22. Quistad SD, Grasis JA, Barr JJ, Rohwer FL. Viruses and the origin of microbiome selection and immunity. ISME J [Internet]. 2017;11(4):835–40. Available from: http://www.nature.com/doifinder/10.1038/ismej.2016.182

23. Oppen MJH Van, Leong J, Gates RD. Coral-virus interactions: A double-edged sword ? SYMBIOSIS. 2009;47:1–8.

24. Correa AMS, Welsh RM, Vega Thurber RL. Unique nucleocytoplasmic dsDNA and +ssRNA viruses are associated with the dinoflagellate endosymbionts of corals. ISME J [Internet]. 2013;7(1):13–27. Available from: http://dx.doi.org/10.1038/ismej.2012.75

25. Lawrence SA, Floge SA, Davy JE, Davy SK, Wilson WH. Exploratory analysis of Symbiodinium transcriptomes reveals potential latent infection by large dsDNA viruses. Environ Microbiol. 2017;19(10):3909–19.

26. Levin RA, Voolstra CR, Weynberg KD, Van Oppen M. Evidence for a role of viruses in the thermal sensitivity of coral photosymbionts. ISME J. 2017;11:808–12.

27. Knowles B, Bonachela JA, Behrenfeld MJ, Bondoc KG, Cael BB, Carlson CA, et al. Temperate infection in a virus–host system previously known for virulent dynamics. Nat Commun [Internet]. 2020;11(1):1–13. Available from: http://dx.doi.org/10.1038/s41467-020-18078-4

28. Montalvo-Proaño J, Buerger P, Weynberg KD, Van Oppen MJH. A PCR-Based Assay Targeting the Major Capsid Protein Gene of a Dinorna-Like ssRNA Virus That Infects Coral Photosymbionts. Front Microbiol. 2017;8(September):1–8.

29. Tomaru Y, Katanozaka N, Nishida K, Shirai Y, Tarutani K, Yamaguchi M, et al. Isolation and characterization of two distinct types of HcRNAV, a single-stranded RNA virus infecting the bivalve-killing microalga Heterocapsa circularisquama. Aquat Microb Ecol. 2004;34(3):207–18.

30. Shi M, Lin XD, Tian J-H, Chen L-J, Chen X, Li C, et al. Redefining the invertebrate RNA virosphere. Nature [Internet]. 2016;540(7634):539–43. Available from: http://dx.doi.org/10.1038/nature20167

31. Domingo E, Sheldon J, Perales C. Viral Quasispecies Evolution. Microbiol Mol Biol Rev. 2012;76(2):159–216.

32. Sanjuán R, Domingo-Calap P. Mechanisms of viral mutation. Cell Mol Life Sci.

2016;73(23):4433–48.

33. Vlok M, Lang AS, Suttle CA. Marine RNA Virus Quasispecies Are Distributed throughout the Oceans. mSphere. 2019;4(2):1–18.

34. Domingo E, Martinez-salas E, Sobrino F, de la Torre JC, Portela A, Ortin J, et al. The quasispecies (extremely heterogeneous) nature of viral RNA genome populations: biological relevance—a review. Gene. 1985;40:1–8.

35. Vignuzzi M, Stone JK, Arnold JJ, Cameron CE, Andino R. Quasispecies diversity determines pathogenesis through cooperative interactions in a viral population. Nature. 2006;439(7074):344–8.

36. Holland J, Spindler K, Horodyski F, Grabau E, Nichol S, Vandepol S. Rapid Evolution of RNA Genomes. Science (80-). 1982;215(4540):1577–85.

37. Gélin P, Postaire B, Fauvelot C, Magalon H. Molecular Phylogenetics and Evolution Reevaluating species number, distribution and endemism of the coral genus Pocillopora Lamarck, 1816 using species delimitation methods and microsatellites. Mol Phylogenet Evol. 2017;109:430–46.

38. Pratchett MS, McCowan D, Maynard JA, Heron SF. Changes in Bleaching Susceptibility among Corals Subject to Ocean Warming and Recurrent Bleaching in Moorea, French Polynesia. PLoS One. 2013;8(7):1–10.

39. Donovan MK, Adam TC, Shantz AA, Speare KE, Munsterman KS, Rice MM, et al. Nitrogen pollution interacts with heat stress to increase coral bleaching across the seascape. Proc Natl Acad Sci U S A. 2020;117(10):5351–7.

40. Siebeck UE, Marshall NJ, Kluter A, Hoegh-Guldberg O. Monitoring coral bleaching using a colour reference card. Coral Reefs. 2006;

41. Winters G, Holzman R, Blekhman A, Beer S, Loya Y. Photographic assessment of coral chlorophyll contents: Implications for ecophysiological studies and coral monitoring. J Exp Mar Bio Ecol [Internet]. 2009;380:25–35. Available from: http://dx.doi.org/10.1016/j.jembe.2009.09.004

42. Hume BCC, Ziegler M, Poulain J, Pochon X, Romac S, Boissin E, et al. An improved primer set and amplification protocol with increased specificity and sensitivity targeting the Symbiodinium ITS2 region. PeerJ. 2018;2018(5):1–22.

43. Howe-kerr LI, Bachelot B, Wright RM, Kenkel CD, Bay LK, Correa AMS. Symbiont community diversity is more variable in corals that respond poorly to stress. Glob Chang Biol. 2020;00:1–15.

44. Hume BCC, Smith EG, Ziegler M, Warrington HJM, Burt JA, LaJeunesse TC, et al. SymPortal: A novel analytical framework and platform for coral algal symbiont next-generation sequencing ITS2 profiling. Mol Ecol Resour. 2019;19(4):1063–80.

45. Veglia AJ, E. Rivera Vicéns R, Grupstra CG, Howe-Kerr LI, Correa AM. vAMPirus: An automated, comprehensive virus amplicon sequencing analysis program [Internet]. 2021. Available from: https://zenodo.org/record/4549851

46. Edgar RC. UNOISE2: improved error-correction for Illumina 16S and ITS amplicon sequencing. bioRxiv [Internet]. 2016;81257. Available from: http://biorxiv.org/lookup/doi/10.1101/081257

47. Rognes T, Flouri T, Nichols B, Quince C, Mahé F. VSEARCH: A versatile open source tool for metagenomics. PeerJ. 2016;2016(10):1–22.

554 48. Edgar RC. MUSCLE: A multiple sequence alignment method with reduced time and space
555 complexity. BMC Bioinformatics. 2004;5:1–19.

556 49. Darriba D, Posada D, Kozlov AM, Stamatakis A, Morel B, Flouri T. ModelTest-NG: A New and
557 Scalable Tool for the Selection of DNA and Protein Evolutionary Models. Mol Biol Evol.
558 2020;37(1):291–4.

559 50. Oksanen J, Blanchet G, Friendly M, Kindt R, Legendre P, McGlinn D, et al. vegan: Community
560 Ecology Package. R package version 2.4-6. R Packag version 25-6. 2019;

561 51. Bates DM, Maechler M, Bolker B, Walker S. lme4: Mixed-effects modeling with R. R Packag
562 version 11-7, http//CRANR-project.org/package=lme4. 2014;

563 52. Anderson MJ, Walsh DCI. PERMANOVA, ANOSIM, and the Mantel test in the face of
564 heterogeneous dispersions: What null hypothesis are you testing? Ecol Monogr. 2013;83(4):557–
565 74.

566 53. Love MI, Huber W, Anders S. Moderated estimation of fold change and dispersion for RNA-seq
567 data with DESeq2. Genome Biol. 2014;15(12):550.

568 54. Rädecker N, Pogoreutz C, Gegner HM, Cárdenas A, Roth F. Heat stress destabilizes symbiotic
569 nutrient cycling in corals. Proceeding Natl Acad Sci United Stated Am.
570 2021;118(5):e2022653118.

571 55. Wham DC, LaJeunesse TC. Symbiodinium population genetics: testing for species boundaries and
572 analysing samples with mixed genotypes. Mol Ecol. 2016;25:2699–712.

573 56. Biebricher CK, Eigen M. What Is a Quasispecies? In: Domingo E, editor. Quasispecies: Concept
574 and Implications for Virology [Internet]. Berlin, Heidelberg: Springer Berlin Heidelberg; 2006. p.
575 1–31. Available from: https://doi.org/10.1007/3-540-26397-7_1

576 57. Gelbart M, Harari S, Ben-ari Y, Kustin T, Wolf D, Mandelboim M, et al. Drivers of within-host
577 genetic diversity in acute infections of viruses. PLoS Pathog [Internet]. 2020;16(11):e1009029.
578 Available from: http://dx.doi.org/10.1371/journal.ppat.1009029

579 58. Correa AMS, Howard-Varona C, Coy SR, Buchan A, Sullvian MB, Weitz JS. The virus-microbe
580 infection continuum: Revisiting the viral rules of life. Nat Rev Microbiol. 2021;1–35.

581 59. Breitbart M, Bonnain C, Malki K, Sawaya NA. Phage puppet masters of the marine microbial
582 realm. Nat Microbiol [Internet]. 2018;3(July). Available from: http://dx.doi.org/10.1038/s41564-
583 018-0166-y

584 60. Mann NH, Cook A, Millard A, Bailey S, Clokie M. Bacterial photosynthesis genes in a virus.
585 Nature. 2003;424(6950):741.

586 61. Marquez LM, Redman RS, Rodriguez RJ, Roossinck MJ. A Virus in a Fungus in a Plant: Three-
587 way Symbiosis required for thermal tolerance. Science (80-). 2007;315(January).

588 62. Holmes EC. The RNA Virus Quasispecies: Fact or Fiction? J Mol Biol [Internet].
589 2010;400(3):271–3. Available from: http://dx.doi.org/10.1016/j.jmb.2010.05.032

590 63. Pybus OG, Rambaut A, Belshaw R, Freckleton RP, Drummond AJ, Holmes EC. Phylogenetic
591 evidence for deleterious mutation load in RNA viruses and its contribution to viral evolution. Mol
592 Biol Evol. 2007;24(3):845–52.

593 64. Holmes EC. Patterns of Intra- and Interhost Nonsynonymous Variation Reveal Strong Purifying
594 Selection in Dengue Virus. J Virol. 2003;77(20):11296–8.

65. Edwards CTT, Holmes EC, Pybus OG, Wilson DJ, Viscidi RP, Abrams EJ, et al. Evolution of the human immunodeficiency virus envelope gene is dominated by purifying selection. Genetics. 2006;174(3):1441–53.

66. Roux S, Hawley AK, Beltran MT, Scofield M, Schwientek P, Stepanauskas R, et al. Ecology and evolution of viruses infecting uncultivated SUP05 bacteria as revealed by single-cell- and meta-genomics. Elife. 2014;3:e03125.

67. Labonté JM, Swan BK, Poulos B, Luo H, Koren S, Hallam SJ, et al. Single-cell genomics-based analysis of virus–host interactions in marine surface bacterioplankton. ISME J. 2015;9:2386–99.

68. Munson-mcgee JH, Peng S, Dewerff S, Stepanauskas R, Whitaker RJ, Weitz JS, et al. A virus or more in (nearly) every cell: ubiquitous networks of virus–host interactions in extreme environments. ISME J [Internet]. 2018;12:1706–14. Available from: http://dx.doi.org/10.1038/s41396-018-0071-7

69. Díaz-Muñoz SL. Viral coinfection is shaped by host ecology and virus-virus interactions across diverse microbial taxa and environments. Virus Evol. 2017;3(1):1–14.

70. Ripp S, Miller R V. The role of pseudolysogeny in bacteriophage-host interactions in a natural freshwater environment. Microbiology. 1997;143(6):2065–70.

71. Onodera S, Olkkonen VM, Gottlieb P, Strassman J, Qiao XY, Bamford DH, et al. Construction of a transducing virus from double-stranded RNA bacteriophage phi6: establishment of carrier states in host cells. J Virol. 1992;66(1):190–6.

72. Wang L, Wu S, Liu T, Sun J, Chi S, Liu C, et al. Endogenous viral elements in algal genomes. Acta Oceanol Sin. 2014;33(2):102–7.

73. Moniruzzaman M, Weinheimer AR, Martinez-Gutierrez CA, Aylward FO. Widespread endogenization of giant viruses shapes genomes of green algae. Nature [Internet]. 2020;588(7836):141–5. Available from: http://dx.doi.org/10.1038/s41586-020-2924-2

74. Ku C, Sheyn U, Sebé-Pedrós A, Ben-Dor S, Schatz D, Tanay A, et al. A single-cell view on alga-virus interactions reveals sequential transcriptional programs and infection states. Sci Adv. 2020;6(21).

75. Deng L, Ignacio-espinoza JC, Gregory AC, Poulos BT, Weitz JS, Hugenholtz P, et al. Viral tagging reveals discrete populations in Synechococcus viral genome sequence space. Nature [Internet]. 2014;513:242–6. Available from: http://dx.doi.org/10.1038/nature13459

76. Jonge PA De, Costa AR, Franklin L, Brouns SJJ, Jonge PA De, Meijenfeldt FAB Von, et al. Adsorption Sequencing as a Rapid Method to Link Environmental Bacteriophages to Hosts. ISCIENCE [Internet]. 2020;23(9):101439. Available from: https://doi.org/10.1016/j.isci.2020.101439

77. Jiang SC, Paul JH. Seasonal and diel abundance of viruses and occurrence of lysogeny/bacteriocinogeny in the marine environment. Mar Ecol Prog Ser. 1994;104(1–2):163–72.

78. Brum JR, Hurwitz BL, Schofield O, Ducklow HW, Sullivan MB. Seasonal time bombs: dominant temperate viruses affect Southern Ocean microbial dynamics. ISME J [Internet]. 2016;10(2):437–49. Available from: http://dx.doi.org/10.1038/ismej.2015.125

79. Winter C, Bouvier T, Weinbauer MG, Thingstad TF. Trade-Offs between Competition and Defense Specialists among Unicellular Planktonic Organisms: the “Killing the Winner” Hypothesis Revisited. Microbiol Mol Biol Rev. 2010;74(1):42–57.

80. Thingstad TF, Våge S, Storesund JE, Sandaa R, Giske J. A theoretical analysis of how strain-specific viruses can control microbial species diversity. PNAS. 2014;111(21).

81. Thingstad TF. Elements of a theory for the mechanisms controlling abundance, diversity, and biogeochemical role of lytic bacterial viruses in aquatic systems. Limnol Oceanogr. 2000;45(6):1320–8.

82. Edgar RS, Lielausis I. Temperature-sensitive mutants of bacteriophage T4D: Their isolation and genetic characterization. Genetics. 1964;49(April):649–62.

83. Vega Thurber RL, Barott KL, Hall D, Liu H, Rodriguez-Mueller B, Desnues C, et al. Metagenomic analysis indicates that stressors induce production of herpes-like viruses in the coral Porites compressa. Proc Natl Acad Sci U S A. 2008;105(47):18413–8.

84. Sadeghi M, Tomaru Y, Ahola T. RNA Viruses in Aquatic Unicellular Eukaryotes. Viruses. 2021;

85. Tomaru Y, Hata N, Masuda T, Tsuji M, Igata K, Masuda Y, et al. Ecological dynamics of the bivalve-killing dinoflagellate Heterocapsa circularisquama and its infectious viruses in different locations of western Japan. Environ Microbiol. 2007;9(6):1376–83.

86. Randall RE, Griffin DE. Within host RNA virus persistence: mechanisms and consequences. Curr Opin Virol [Internet]. 2017;23(August):35–42. Available from: http://dx.doi.org/10.1016/j.coviro.2017.03.001

87. Roossinck MJ. Lifestyles of plant viruses. Philos Trans R Soc B Biol Sci. 2010;365(1548):1899–905.

88. Honjo MN, Emura N, Kawagoe T, Sugisaka J, Kamitani M, Nagano AJ, et al. Seasonality of interactions between a plant virus and its host during persistent infection in a natural environment. ISME J [Internet]. 2020;14(2):506–18. Available from: http://dx.doi.org/10.1038/s41396-019-0519-4

89. Kim Y, Kim YJ, Paek K-H. Temperature-specific vsiRNA confers RNAi-mediated viral resistance at elevated temperature in Capsicum annuum . J Exp Bot. 2020;72(4):1432–48.

90. Jones RAC. Future Scenarios for Plant Virus Pathogens as Climate Change Progresses [Internet]. 1st ed. Vol. 95, Advances in Virus Research. Elsevier Inc.; 2016. 87–147 p. Available from: http://dx.doi.org/10.1016/bs.aivir.2016.02.004

91. Brüwer JD, Agrawal S, Liew YJ, Aranda M, Voolstra CR. Association of coral algal symbionts with a diverse viral community responsive to heat shock. BMC Microbiol. 2017;17(1):1–11.

92. Cevallos RC, Sarnow P. Temperature Protects Insect Cells from Infection by Cricket Paralysis Virus. J Virol. 2010;84(3):1652–5.

93. Lohr J, Munn CB, Wilson WH. Characterization of a latent virus-like infection of symbiotic zooxanthellae. Appl Environ Microbiol. 2007;73(9):2976–81.

94. Weynberg KD, Levin RA, Neave MJ, Clode PL, Voolstra CR, Brownlee C, et al. Prevalent viral infection in cultures of the coral algal endosymbiont,. Coral Reefs. 2017;

95. Seifert M, van Nies P, Papini FS, Arnold JJ, Poranen MM, Cameron CE, et al. Temperature controlled high-throughput magnetic tweezers show striking difference in activation energies of replicating viral RNA-dependent RNA polymerases. Nucleic Acids Res. 2020;48(10):5591–602.

96. Wooldridge SA. Differential thermal bleaching susceptibilities amongst coral taxa: Re-posing the role of the host. Coral Reefs. 2014;33(1):15–27.

678 97. Guest JR, Baird AH, Maynard JA, Muttaqin E, Edwards AJ, Campbell SJ, et al. Contrasting
679 patterns of coral bleaching susceptibility in 2010 suggest an adaptive response to thermal stress.
680 PLoS One. 2012;7(3):e33353.

681

682

Figure legends

Figure 1 Representative examples of Symbiodiniaceae cells in *Pocillopora* species complex coral fragments in control (a-b) and heat (c-f) treatments after 24 hours, as well as examples of virus-like particles (VLPs) associated with these Symbiodiniaceae cells. Some Symbiodiniaceae cells in heat-treated coral fragments exhibited vacuolization, unlike cells in control fragments (a-b). Many vacuoles contained VLPs (c-f). Most observed VLPs had icosahedral, electron-dense capsids that ranged from 110-170 nm in diameter and lacked an envelope. Many VLPs appeared to be endocytosed by—or exiting—Symbiodiniaceae cells (d-f), and some VLPs were visible outside Symbiodiniaceae cells (c). (d) is an enlargement of (c). Arrows indicate VLPs. C: Symbiodiniaceae cell chloroplast; N: Symbiodiniaceae cell nucleus; P: *Pocillopora* species complex coral tissue; S: Symbiodiniaceae cell starch grain; V: Vacuole.

695 **Figure 2** Maximum likelihood tree of major capsid protein (*mcp*) aminotypes (unique
696 amino acid sequences) from Symbiodiniaceae-infecting dinoRNA viruses ('dinoRNAVs')
697 isolated from five coral colonies of *Pocillopora* species complex. Aminotypes recovered in this
698 study were similar to those reported in a previous work that isolated dinoRNAV sequences from
699 6 coral species via similar methods (28). Black dots at nodes represent bootstrap support >75%.
700 Colors adjacent to the tree indicate the study (orange, purple) or NCBI reference (blue) for each
701 *mcp* aminotype. Reference NCBI accession numbers are: Beihai Sobemo-like Virus 4
702 (YP_009336877), Sponge Weivirus-like Virus 6 (ASM94037), Cladocopium Virus i2
703 (AOS87317), Cladocopium Virus i1 (AOG17586), HcRNAV-CY (BAE47072), HcRNAV-UA
704 (BAE47070) and HcRNAV-659 (BAU51723). Rings with black or red squares indicate the
705 relative, log(10)-transformed abundances of dinoRNAV aminotype in fragments from individual
706 coral colonies in the control or heat treatment, respectively. Aminotypes labeled with *PVID* and a
707 numeral comprise >1% abundance of the total dataset and are included in Figure 3. Black and
708 red asterisks indicate aminotypes that were significantly associated with control or heat
709 treatments, respectively (see Figure 5 for details).

710

711 **Figure 3** Overview of Symbiodiniaceae-infecting dinoRNAV major capsid protein (*mcp*)
712 gene aminotypes (unique amino acid sequences) associated with five colonies of the stony coral
713 *Pocillopora* species complex. (a) Venn diagram indicating that ~82% (102) of 124 unique
714 aminotypes were shared between coral colonies. Non-rarified data for each colony ranges from
715 8-11 fragments sampled from control and heated aquaria. The total number of aminotypes
716 detected per colony is given in parentheses. (b) The relative abundances of *mcp* aminotypes
717 differed in fragments exposed to a ~2 ˚C temperature increase ('Heat' treatment), compared to
718 fragments from the same colonies exposed to ambient reef conditions ('Control'). Empty bars
719 correspond to samples that had <10 000 reads and were excluded from the analysis.
720 PERMANOVA results: Coral colony R^2 = 0.762, $p<0.001$; Treatment R^2= 0.024, $p<0.001$;
721 Treatment*Coral colony R^2=0.068, $p<0.001$; Time R^2= 0.014, $p>0.05$.

722

723 **Figure 4** Diversity of Symbiodiniaceae-infecting dinoRNAV major capsid protein (*mcp*)
724 gene aminotypes (unique amino acid sequences) in heat ('Heat', 'H') versus control ('Control',
725 'C') conditions. (a) Venn diagram of non-rarified aminotypes in heat and control treatments.
726 Seventeen unique aminotypes were detected in coral fragments exposed to heat, compared to 1
727 unique aminotype in control fragments. (b, h) Diversity (Shannon's diversity index, H) of
728 aminotypes increased in fragments exposed to heat compared to control fragments, and over time
729 (d, h); variation also appeared to occurr among colonies (f). (c, i) Estimated aminotype richness
730 increased in fragments exposed to heat, but not over time (e, i). (g) Mean aminotype richness
731 also appeared to vary among colonies. Linear mixed effects model (LMM) results for Shannon's
732 diversity index (h) and estimated richness (i). Shannon's diversity index values were based on
733 sequencing data rarefied to 59 837 amino acid sequences per sample; richness was estimated by
734 repeated random subsampling of unrarified data.

735

736 **Figure 5** Differentially abundant Symbiodiniaceae-infecting dinoRNAV major capsid
737 protein (*mcp*) aminotypes (unique amino acid sequences) across the experiment. Twenty-eight
738 viral aminotypes (each represented as a point with a unique shape and color) were differentially
739 abundant across control and heated *Pocillopora* species complex coral fragments. Of these, 22
740 aminotypes occurred at higher relative abundances in heat-treated fragments (right of the 0 lines)
741 and 6 had higher relative abundances in control fragments (left of the 0 lines). Ten aminotypes
742 were differentially abundant at multiple (2-4) timepoints throughout the experiment. This
743 analysis was conducted using DeSeq2 on a non-rarefied dataset. DESeq2 analyses were run
744 separately for each time point ($t_{(h)}$= 4, 12, 24, 72, 108, see Methods for more details).

745

746 **Figure 6** Dispersion of Symbiodiniaceae-infecting dinoRNAV major capsid protein (*mcp*)
747 gene aminotypes (unique amino acid sequences) associated with *Pocillopora* species complex
748 coral fragments in heat-treated (H) versus control (C) conditions. (a) A non-metric
749 Multidimensional Scaling (nMDS) plot depicts that dinoRNAVs differ by coral colony ID, and
750 to a lesser extent, treatment. (b) Dispersion of dinoRNAV aminotypes was higher in heat-treated
751 fragments. (c) Mean (±SE) aminotype dispersion was consistently higher over time in heat-
752 treated fragments and (d) varied among coral colonies. (e) Results of a linear mixed effects
753 model testing the effect of treatment and time on dispersion. Centroids were calculated
754 separately for each colony in control and heat-treated conditions based on Bray-Curtis distances
755 from square-root-transformed rarefied data. Dispersion was quantified by measuring the distance
756 of each sample to its centroid.

757

Table 1 Summary of studies in which Symbiodiniaceae-infecting dinoflagellate RNA virus (dinoRNAV) genes have been recovered from coral colonies or Symbiodiniaceae cultures. Samples sizes are n=1 unless otherwise indicated in parentheses. **Bolded** Symbiodiniaceae types were directly identified in a given study. All other Symbiodiniaceae listed represent the genera typically reported from each coral species based on published literature.

Sample type	***Symbiodiniaceae genus or species (detected or reported in literature)***	***Collection location***	***DinoRNAV detection method***	***Notes***	***Reference***
Coral holobiont					
Montastrea cavernosa (4)	*Cladocopium*[a]	Key West, FL	Viral particle isolation, 454 pyrosequencing	DinoRNAVs detected in heat-treated corals.	Correa et al. 2013
Acropora tenuis	*Cladocopium*[b]	Orpheus Island, Central GBR	Viral particle isolation, RP-SISPA, MiSeq sequencing.	DinoRNAVs ≥99% of ssRNA viruses detected from pooled tissue of 3 colonies. No dinoRNAVs detected in *Pocillopora damicornis*.	Weynberg et al. 2014
Acropora tenuis *Fungia fungites* *Galaxea fascicularis* *Pocillopora damicornis* *Porites cylindrica* *Porites lutea* (6)	*Cladocopium*[b] *Cladocopium*[b] *Cladocopium* or *Durusdinium*[b] *Cladocopium*[b] *Cladocopium*[b] ***Cladocopium* C15**	Davies Reef and Orpheus Island, Central GBR	Viral particle isolation, targeted PCR assay, MiSeq sequencing.	DinoRNAVs not detected in *Acropora hyacinthus*, *Acropora millepora* or *Goniastrea aspera*.	Montalvo-Proaño et al. 2017
Acropora tenuis *Fungia fungites* *Galaxea fascicularis*	*Cladocopium*[b] *Cladocopium*[b] *Cladocopium* or *Durusdinium*[b]	Orpheus Island, Central GBR	Viral particle isolation, RP-SISPA, MiSeq sequencing.	Corals collected in triplicate and pooled prior to sequencing. DinoRNAVs not detected in *Goniastrea aspera*, *Pocillopora acuta*, *Pocillopora damicornis*, or *Pocillopora verrucosa.*	Weynberg et al. 2017
Symbiodiniaceae culture					
Cladocopium C1 (2)	***Cladocopium* C1**	Magnetic Island and South Molle Island,	HiSeq sequencing of poly(A)-purified RNA.	Culture originally isolated from *Acropora tenuis.* Higher expression of dinoRNAV major capsid protein genes in a thermo-	Levin et al. 2017

	Central GBR	sensitive *Cladocopium* strain under ambient temperatures.

[a] Serrano et al. 2014

[b] Tonk et al. 2013

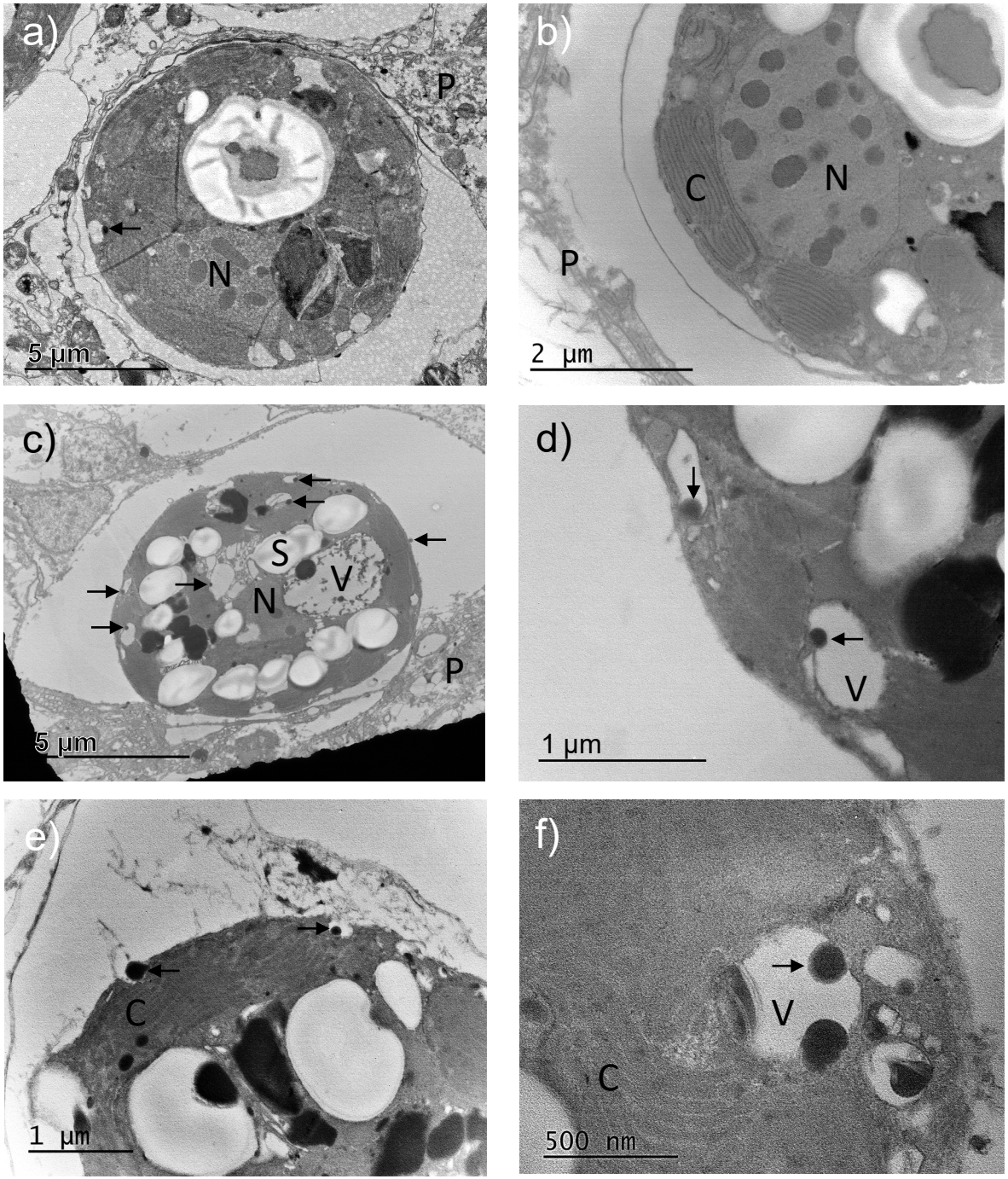
a)
P
N
5 µm
b)
C
N
P
2 µm
c)
S
V
N
P
5 µm
d)
V
1 µm
e)
C
1 µm
f)
V
C
500 nm

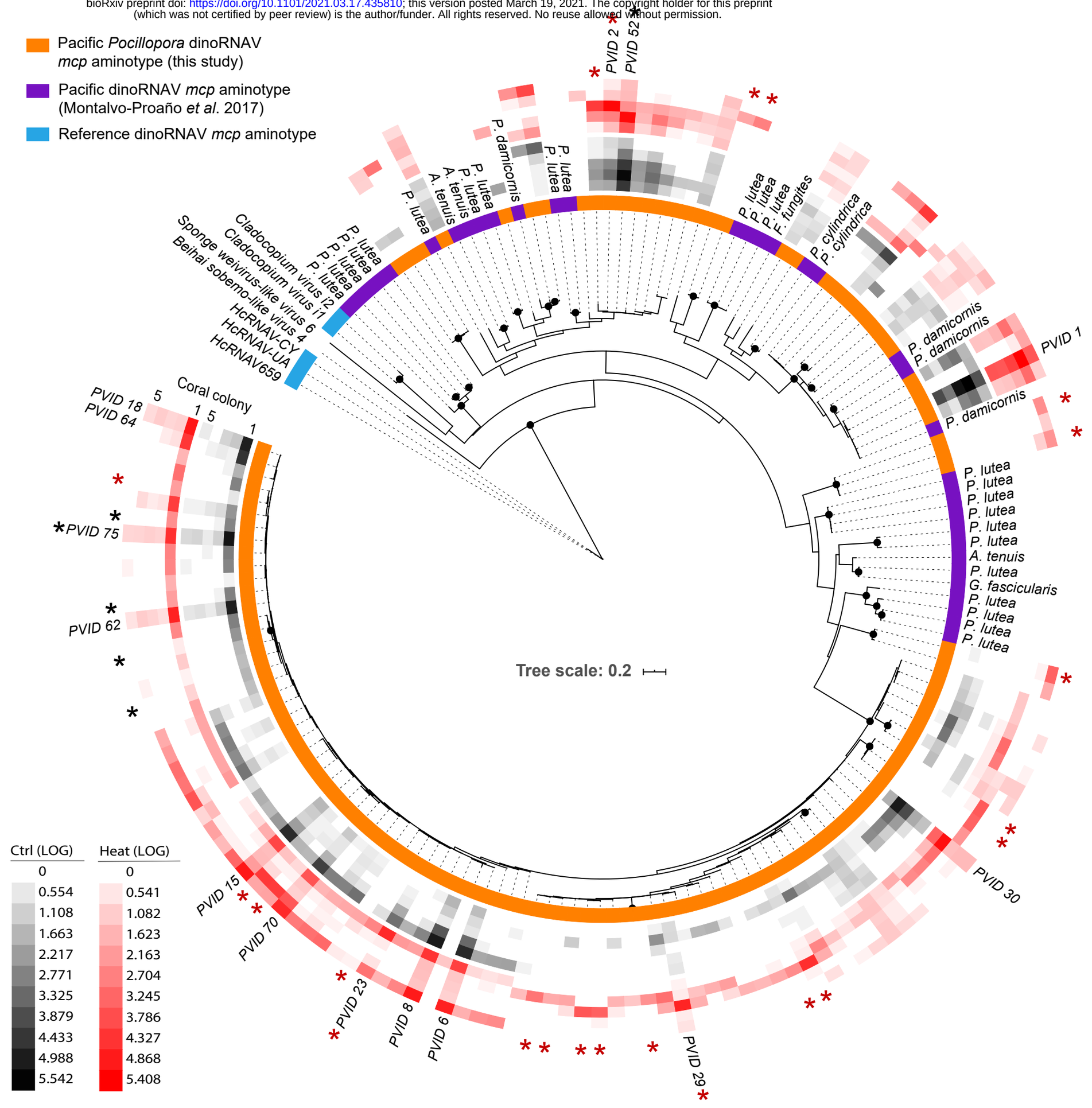

a

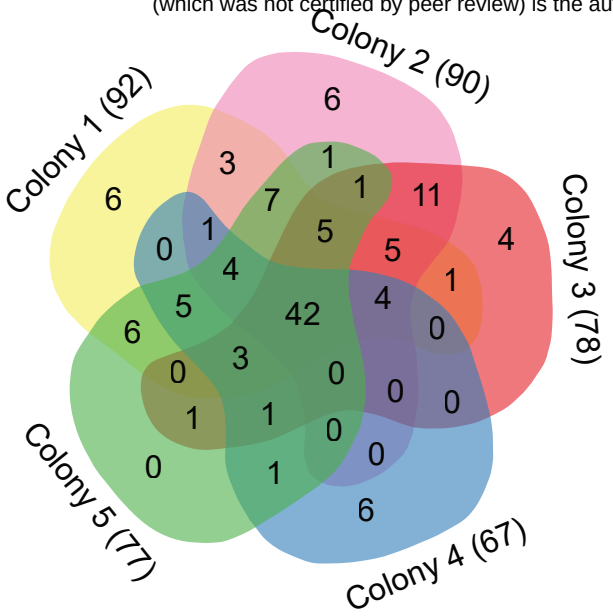

b

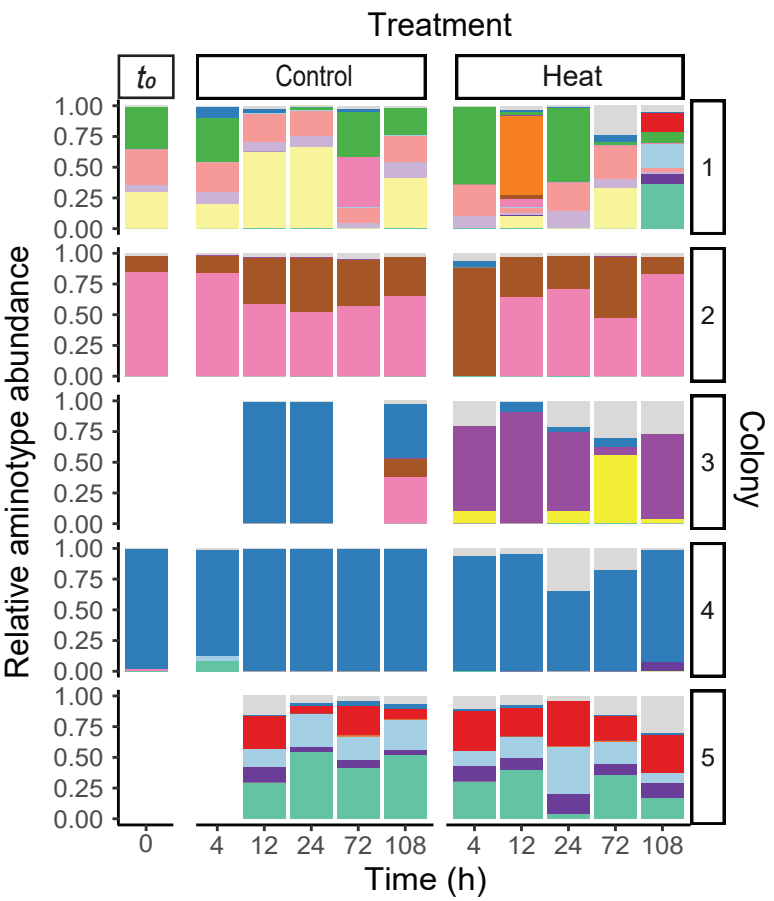

Aminotypes

- Other < 1%
- PVID_AminoType1
- PVID_AminoType15
- PVID_AminoType18
- PVID_AminoType2
- PVID_AminoType23
- PVID_AminoType29
- PVID_AminoType30
- PVID_AminoType52
- PVID_AminoType6
- PVID_AminoType62
- PVID_AminoType64
- PVID_AminoType70
- PVID_AminoType75
- PVID_AminoType8

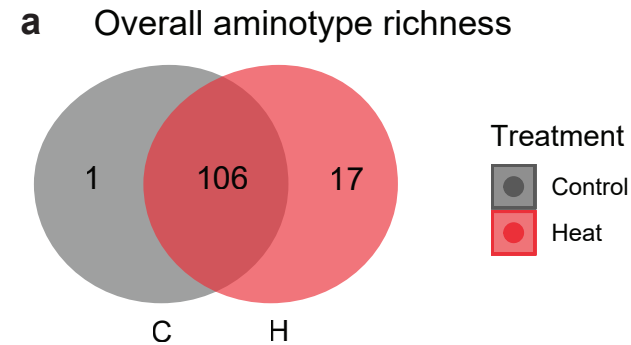

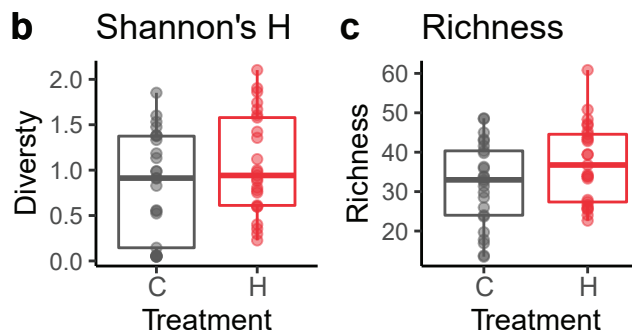

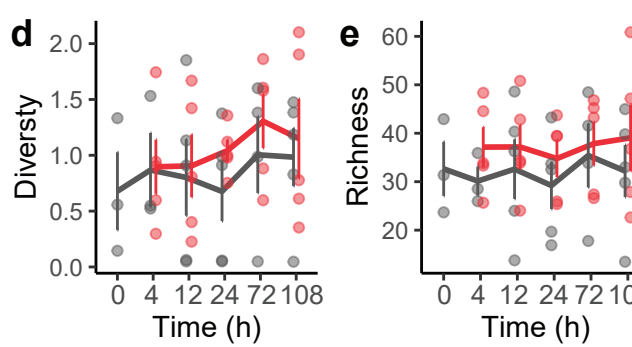

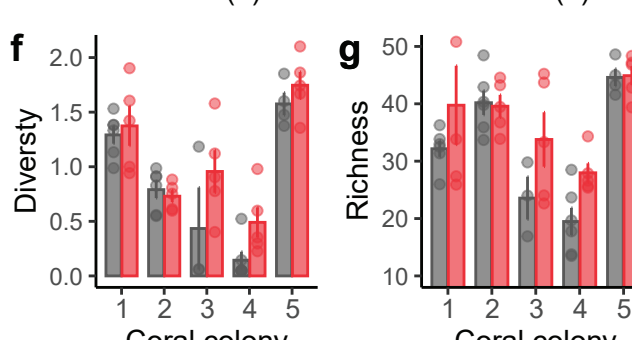

h

LMM results:

Treatment	**p<0.05**
Time	**p<0.05**
Treatment*Time	p>0.05

i

LMM results:

Treatment	**p<0.05**
Time	p>0.05
Treatment*Time	p>0.05

Table 2 Summary of observations, relative abundance and identity of Symbiodiniaceae-infecting dinoRNAV aminotypes (unique amino acid sequences) specific to heat or control fragments in this study. 'Colony' indicates the coral colony IDs in which a given aminotype was detected. 'N_Observations' lists the total number of fragments in which a given aminotype was observed. 'Time observed (h)' lists the sampling timepoints at which an aminotype was detected. 'Mean relative abundance (%)' indicates the mean relative abundance of an aminotype across the fragments from which it was detected. 'Closest match' lists the strongest similarity of an aminotype in this study to known or putative viruses based on BLASTx against a reference database containing all sequences from the reference viral database (Goodacre et al., 2018) and the aminotypes generated from reprocessed Montalvo-Proaño et al. (2017) data.

Aminotype ID	*Colony*	*N_Observations*	*Time observed (h)*	*Mean relative abundance (%)*	*Closest match*
Heat treatment					
22	4	3	12,24,72	0.048	Plutea_AminoType17
25	3	2	24,72	1.766	Plutea_AminoType21
37	2	1	4	0.098	Plutea_AminoType21
44	1	2	4,12	0.013	Plutea_AminoType13
68	2,3	4	4,24,72	0.016	Plutea_AminoType21
72	3	1	4	0.021	Pdamicornis_AminoType1
76	1,2,5	5	4,12,24,72	0.026	Plutea_AminoType13
80	2	1	108	0.033	Plutea_AminoType21
81	4	1	108	0.027	Plutea_AminoType5
87	4	1	24	0.019	Plutea_AminoType10
104	3	2	24,72	0.162	Plutea_AminoType21
107	4	3	24,72,108	0.035	Gfascicularis_AminoType1
112	4	4	12,24,72,108	0.217	Plutea_AminoType17
114	3	1	72	1.380	Plutea_AminoType4
115	2,3	2	4,72	0.684	Plutea_AminoType21
117	2	1	108	0.375	Plutea_AminoType21
118	4	1	4	0.376	Plutea_AminoType10
Control treatment					
91	2	1	72	0.019	Plutea_AminoType4

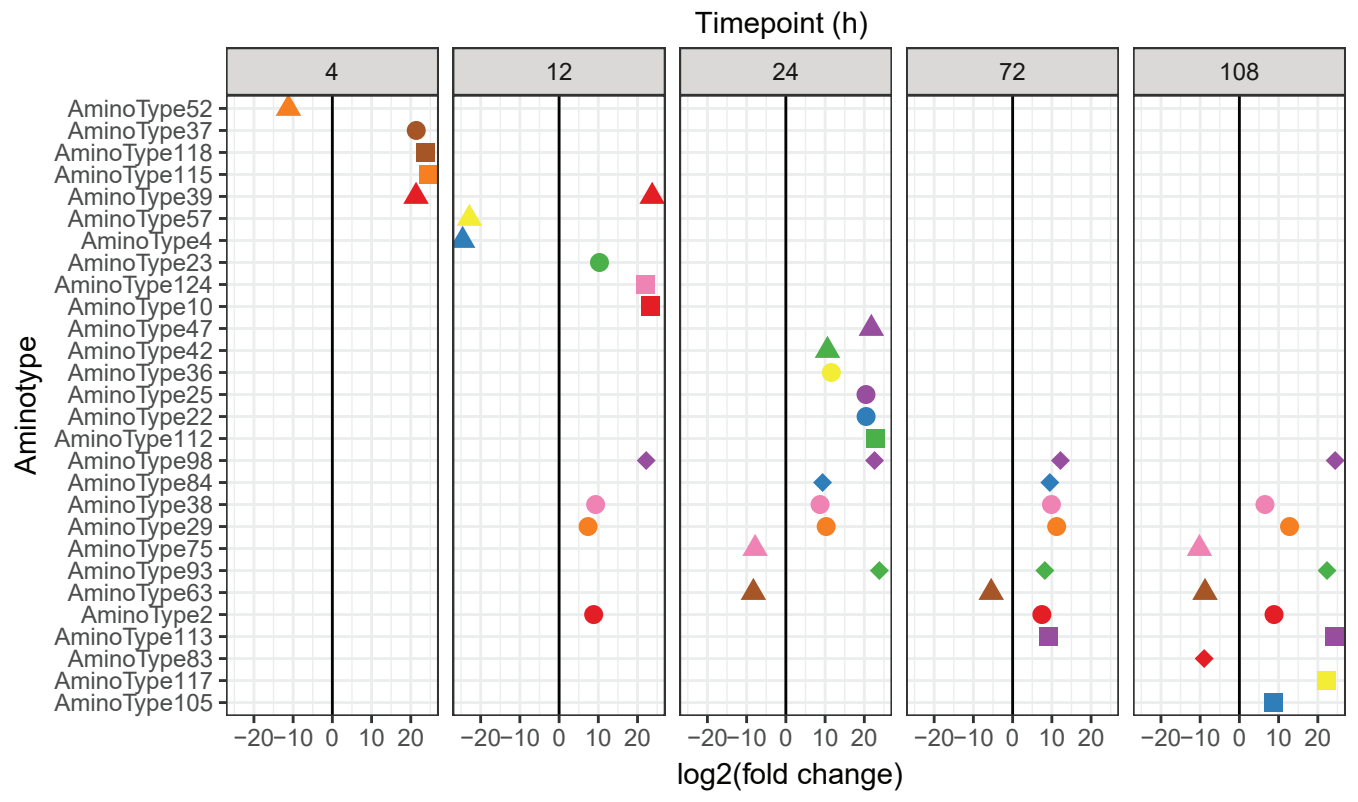
Timepoint (h)
4
12
24
72
108
Aminotype
AminoType52
AminoType37
AminoType118
AminoType115
AminoType39
AminoType57
AminoType4
AminoType23
AminoType124
AminoType10
AminoType47
AminoType42
AminoType36
AminoType25
AminoType22
AminoType112
AminoType98
AminoType84
AminoType38
AminoType29
AminoType75
AminoType93
AminoType63
AminoType2
AminoType113
AminoType83
AminoType117
AminoType105
−20 −10 0 10 20
log2(fold change)

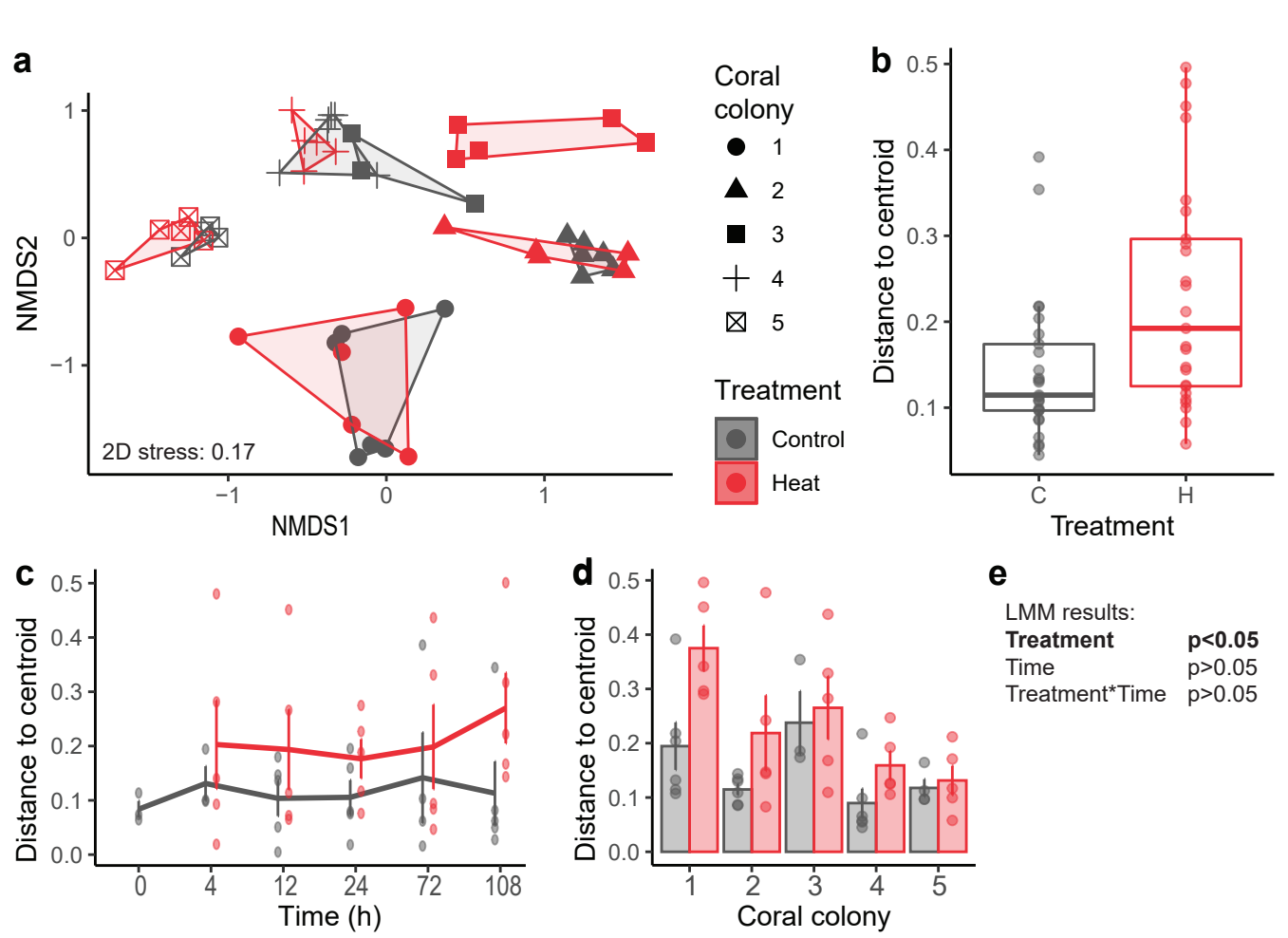
a
NMDS2
NMDS1
2D stress: 0.17
Coral colony
1
2
3
4
5
Treatment
Control
Heat
b
Distance to centroid
C
H
Treatment
c
Distance to centroid
Time (h)
d
Distance to centroid
Coral colony
e
LMM results:
Treatment p<0.05
Time p>0.05
Treatment*Time p>0.05